A novel metal organic framework (MOF) - mediated interfacial polymerization for direct deposition of polyamide layer on ceramic substrates for nanofiltration

*Yueping Bao, Yunfeng Chen, Teik-Thye Lim, Rong Wang and Xiao Hu**

Yueping Bao

Interdisciplinary Graduate School, Nanyang Technological University, 639798, Singapore;

Yueping Bao; Dr. Yunfeng Chen; Prof. Teik-Thye Lim; Prof. Rong Wang; Prof. Xiao Hu

Nanyang Environment and Water Research Institute, Nanyang Technological University, 637141, Singapore.

Prof. Teik-Thye Lim; Prof. Rong Wang;

School of Civil and Environmental and Engineering, Nanyang Technological University, 639798, Singapore.

Prof. Xiao Hu

School of Materials Science and Engineering, Nanyang Technological University, 639798, Singapore

E-mail: ASXHU@ntu.edu.sg.

Keywords: reactive-seeded growth, MOF-mediated, interfacial polymerization, organic-inorganic composites

Abstract

A facile metal-organic framework (MOF)-mediated interfacial polymerization (IP) method has been developed to prepare a polyamide (PA) layer directly on the ceramic substrate for nanofiltration. MOF was introduced to connect ceramic substrate and PA layer via chemical bonding, resulting in a robust separation layer. The optimization of IP could be controlled by MOF growth process via tuning the surface roughness as well as hydrophilicity. This method would provide a new way for the preparation of next generation of organic-inorganic composite membranes.

Ceramic membranes have drawn increasing attention due to their excellent chemical and physical properties. Meanwhile, they have been considered as an attractive alternative to polymer membranes when considering the social sustainability [1,2]. However, the limitation on selectivity for ceramic membranes results in their application restricted to microfiltration and ultrafiltration [3]. It is still a challenge to fabricate a robust ceramic membrane for nanofiltration [4,5].

On the other hand, polyamide (PA) membrane, which could be formed via interfacial polymerization (IP), has shown high stability and selectivity in reverse osmosis [6,7]. Up to now, lots of work have been finished to fabricate a PA selective layer on polymeric support for water treatment [8–11]. However, limited studies have been focused on preparing thin selective layers via IP on porous ceramic substrates [12,13], which might be caused by the relatively rough surface of ceramic membranes as well as the weak interaction between organics and inorganics. Generally, an inter-grown polymeric intermediate layer would be needed to facilitate the IP fabrication on ceramic substrates [12,14]. However, the weak physical connection between the substrate and the selective layer makes the membrane not stable nor robust, especially in high pressure filtration system, like nanofiltration. It would be a great opportunity to grow a robust PA layer on ceramic substrate as the next-generation composite membrane for the high-pressure filtration application.

When organic-inorganic composites were taken into account, metal-organic frameworks (MOFs) is surely to be one good example in which organic and inorganic structures are well-connected [15]. MOFs are usually synthesized by combining a hydrated metal salt and organic linker using hydrothermal or solvethermal method [16]. Therefore, it is possible to link the MOF layer and the ceramic substrate by chemical reaction followed by PA layer formation via IP.

Our hypothesis for this work is to synthesize a robust PA selective layer on Al_2O_3 ceramic substrates via chemical bonding. It could be achieved by direct IP process with the

assistance of a well-known Al-based MOF structure MIL-53 (Al) ($Al(OH)(C_6H_4(COO)_2)$) as the intermediate connection layer (**Figure 1**). The chemical bonding between MIL-53 and PA layer could be formed via hydrogen bond and dehydration condensation (**Figure S2**). The chemical connection of the composite membrane was investigated and the membrane performance (pure water flux and rejection) was tested. This method would provide a new idea to make organic-inorganic composite membranes for water treatment.

To investigate the MIL-53 growth mechanism, the particles prepared at different hydrothermal hours were collected and characterized. XRD patterns (**Figure S4**) show that at the seed growth stage (Stage I), the organic linker could be re-crystalized and is identified as H_2BDC ($C_8H_6O_4$, benzene-1,4-dicarboxylic acid, Entry No. 00-021-1919). At the MIL-53 growth stage (Stage II), pure MIL-53 crystals could be generated, all peaks in the XRD patterns can be matched well with the simulated patterns (Entry No. 00-067-0849, **Figure S5**). Even the hydrothermal growth time has no significant effect on the crystal structure, it does affect the morphology and the crystal size of MIL-53 powders observed from FESEM images (**Figure S6**).

The XRD patterns and FTIR spectra (**Figure 2 g and h**) of M-4 show that MIL-53 layer was successfully formed on Al_2O_3 substrate. Meanwhile, the insignificant signal difference between M-4 and PA/M-4 membrane may indicate an ultrathin PA layer was formed during IP process, which could be further estimated from FESEM image (**Figure S7**). Moreover, the XRD pattern and FTIR spectra of M-4 show that it contains a full MIL-53 phase comparable with the pure MIL-53 powder (**Figure S4**). To further confirm the successful formation of PA layer on MIL-53 surface, the MIL-53 particle instead of MIL-53 membrane was characterized (**Figure S8**). The new peak at 19° in XRD patterns can be identified as polyamide and the vibration at 2800-2900 cm^{-1} in FTIR could be caused by CH_2 stretch in polyamide. Furthermore, the XPS wide scan confirmed the existence of N in PA/MIL-53 (Al), evidencing the PA layer formation on MIL-53 (Al) surface.

The effect of hydrothermal growth hours of MIL-53 on morphology of M-X was investigated (**Figure 2**). Results showed that the surface morphology as well as hydrophilicity of the substrates can be controlled by tuning the MOF growth process, which can also be verified by previous research [17]. The seed particles with small size are evenly distributed on the surface of the support due to the connection between H_2BDC and Al on the substrate surface (**Figure S9**). The initial membrane (M-control) shows a porous surface (**Figure 2a**). The M-2 still shows a porous surface and some MIL-53 crystals are observed on the membrane surface (**Figure 2b**). With increasing the hydrothermal time, the crystals grow bigger on the Al_2O_3 substrate surface, resulting a less-porous and smoother surface (M-4). However, when the hydrothermal growth time was further increased, the growth of the MIL-53 crystals became random and promoted the formation of irregular shaped crystals (**Figures 2c-f**), producing a much rougher surface (**Figure S10**). The relatively rough surface might be not favorable for the IP process due to the lack of a smooth and continuous surface. Meanwhile, the cross-sections of MIL-53 (Al) membranes show that a high degree of inter-grown MIL-53 layer which is well bonded with the Al_2O_3 substrate was obtained (**Figure S11**). Compared with the MIL-53 powders prepared at the same conditions, the morphology on the membrane surface changes due to the energy distribution difference.

Figure 3 shows the surface morphologies of PA/M-X membranes. It is quite difficult to form a PA layer directly on the Al_2O_3 membrane surface (PA/M-control) (**Figure 3a**) because of its large pore size as well as high roughness. While, even the porous surfaces were still observed in M-2 (**Figure 2b**), the PA/M-2 membrane shows a dense surface, indicating that the PA layer formed on the M-2 surface (**Figure 3b**). Similar results can be observed in PA/M-X (X=4, 6 and 8) with increased surface roughness. For M-12, no continuous PA layer could be formed on the surface (PA/M-12**)** because of the discontinuous interface caused by its high roughness. The results show that the surface roughness is a critical parameter on the PA layer formation in IP process and it could be controlled by the hydrothermal growth time of MIL-53

layer. Another reason for the unsuccessful IP process for M-12 might be the hydrophobic surface. The M-X membranes gradually become more hydrophobic with extended MIL-53 crystal growth duration. The tested contact angles are 62º, 89º, 107º, 116º and 127º for M-2, M-4, M-6, M-8 and M-12, respectively (**Figure 2**). In a standard IP process, the MPD ($C_6H_8N_2$, *m*-phenylenediamine) solutions could uniformly distributed on the substrate surface and a continuous polyamide could thus be formed at the interface between the aqueous and organic phases [18,19]. Nonetheless, MPD tends to aggregate at the M-X membrane surfaces with increasing surface hydrophobicity during the air gun purging process, thus resulting higher possibility of polyamide failures, or more defects are expected during polyamide formation [20].

As shown in **Figure S12,** the surface roughness decreased from around 450 nm (PA/M-Control) to 340 nm for PA/M-4, which means a smoother polyamide layer was formed on the substrate surface. However, when the hydrothermal time increased from 6 h to 12 h, the surface roughness increased from 431 nm (PA/M-6) to 607 nm (PA/M-12), even higher than the initial one. The results show that the hydrothermal growth time is curial to control the crystal size as well as the surface roughness.

The pure water permeability as well as Rhodamine B (molecule weight of 479) rejection were tested in a home-made dead-end membrane filtration system (**Figure S3**). For PA/M-X membranes, the pure water flux decreases from 57 to 1 LMHB with increasing X from 2 to 12 h (**Figure 3g**). The water permeability primarily depends on the membrane structure including pore size and membrane thickness as well as the surface hydrophilicity [21]. With increasing the hydrothermal growth time, the thickness of MIL-53 layer increases (**Figure S11**) accompanying with the decreasing of pore size, resulting the dramatically decrease of pure water flux (**Figure S13**). Meanwhile, after the formation of PA layer, the flux of PA/M-X membrane were slightly decreased compared with M-X (**Figure 3g**). In the meantime, with the prolonged hydrothermal time, the flux change can be ignored for $X \geq 4$. The results show that the decreased flux was caused by the formation of dense MIL-53 layer on the Al_2O_3 surface.

On the other hand, in the rejection experiment, PA/M-4 shows the highest rejection ratio (>99%), while PA/M-12 only shows a 3.5% rejection, meaning the rejection was caused by the PA layer on the surface, which further confirmed the unsuccessful formation of PA layer on M-12. The color changes of RhB in the permeate side is shown in **Figure 3h**. Furthermore, PA/M-4 also shows a rejection rate of 50.3 % and 20.2 % for $MgSO_4$ and NaCl (**Figure S14**). The long-term test of PA/M-4 was investigated in a 90 min continus filtration, in which the permeate flux decreased dramatically from around 30 to less than 4 LMHB while the rejection for 100 mg L^{-1} RhB solution maintained at > 99%. The decrease of flux could be caused by the RhB cake layer formation on the membrane surface. The high separation performance was comparable with reported study [21], while the chemical bonding in the as-prepared composite membrane make it more robust and stable.

To further verify the versatility of this method, another Al-based MOF (MIL-96) was investigated. The preparation is similar compared with the MIL-53 except H_3BTC ($C_9H_6O_6$, benzene-1,3,5-tricarboxylic acid) was used as the organic linker instead of H_2BDC and the hydrothermal temperature was set at 210 ℃. The results showed the continuous formation of PA layer on the surface could be controlled by the growth of MIL-96 layer (**Figure S15**). Therefore, the idea using MOF as the connected inter-layer would open possibilities for preparation of a thin organic layer onto inorganic substrate. The MOF layer works as a perfect hybrid material to change the pore size and hydrophilicity of the ceramic membrane, forming a surface densified layer and promoting wetting properties for the IP process. Meanwhile, it can form the robust separation layer because of the chemical connection between MOF layer and the substrate. Results showed that the surface roughness which is critical for the IP process could be controlled during the MOF layer growth process. The water permeability was controlled by the formation of MOF layer while the high rejection was enabled by the PA selective layer.

Experimental Section

All chemicals used in the experiment are listed in **Text S1.** The schematic of the MOF-mediate IP method is shown in **Figure 1**. To grow a uniform seed layer of MIL-53 (Al), Al_2O_3 ceramic substrate instead of $Al(NO_3)_3•9H_2O$ was firstly chosen as the Al source. The sample holder (**Figure S1**), which was used to fix the substrate, was put into the autoclave in which the polished surface was faced up followed by the adding of H_2BDC (0.36 g) and DI water (25 g). The autoclave was heated at 220°C for 12 h for the seed growth, in which the organic linker of H_2BDC would react with Al on the substrate surface to form a uniform and thin seed layer (Stage I). After the seeding growth, MIL-53 layer was grown under the similar condition whereby $Al(NO_3)_3•9H_2O$ (0.82 g) was added as the Al source followed by the addition of 0.18 g H_2BDC and 25 g DI water (Stage II). In the MIL-53 growth process, the substrate surface roughness as well as crystal size would be controlled by changing the hydrothermal growth time (2-12 h). After the MOF layer growth, the as-prepared MIL-53/Al_2O_3 membranes were named as M-X, where X represents the growth hours of MIL-53 layer. After the formation of MIL-53 layer on the Al_2O_3 substrate, the M-X membranes were washed with DI water and dried at 100°C overnight for the following IP process. The powders were also collected from the mother solution for the later characterization.

During the IP process, M-X membranes were firstly immersed in the as-prepared aqueous phase (2 w.t% MPD in DI water) for 2 min, after removal of the excess aqueous solution on the membrane surface via air gun purging, the wet membranes were immersed in the as-prepared organic phase (0.1 w.t% TMC in *n*-hexane) for 30 s followed by curing at 60°C for 2 min. The resulted membrane was named as PA/M-X, where X indicates the growth time of MIL-53 layer. After the MOF layer growth, the hydroxyl group (-OH) on the MOF surface can react with amine group (-NH) in MPD via hydrogen bond. Meanwhile, the carboxyl group (-COOH) on residual H_2BDC allows covalent functionalization with -NH by a dehydration

condensation reaction followed by the polyamide formation on the interface (**Figure S2**). To confirm that the synthesis of PA layer on the MOF-53 (Al) surface, direct IP on MOF-53 (Al) powders was conducted.

The as-prepared PA/M-X membranes were characterized (**Text S2**) and the performance was evaluated in a dead-end membrane filtration system (**Text S3**).

References

[1] A. J. Burggraaf, in *Membrane Science and Technology*, Elsevier, **1996**, pp. 21–34.

[2] M. M. Pendergast, E. M. Hoek, *Energy & Environmental Science* **2011**, *4*, 1946.

[3] R. Mallada, M. Menéndez, *Inorganic Membranes: Synthesis, Characterization and Applications*, Elsevier, **2008**.

[4] A. Alem, H. Sarpoolaky, M. Keshmiri, *Ceramics International* **2009**, *35*, 1837.

[5] R. Goei, T.-T. Lim, *Water research* **2014**, *59*, 207.

[6] M. J. Raaijmakers, N. E. Benes, *Progress in polymer science* **2016**, *63*, 86.

[7] W. J. Lau, A. F. Ismail, N. Misdan, M. A. Kassim, *Desalination* **2012**, *287*, 190.

[8] W. Fang, L. Shi, R. Wang, *Journal of membrane science* **2014**, *468*, 52.

[9] X. Wei, S. Wang, Y. Shi, H. Xiang, J. Chen, B. Zhu, *Desalination* **2014**, *350*, 44.

[10] A. K. Ghosh, B.-H. Jeong, X. Huang, E. M. Hoek, *Journal of Membrane Science* **2008**, *311*, 34.

[11] M. Elimelech, W. A. Phillip, *science* **2011**, *333*, 712.

[12] G. M. Shi, T.-S. Chung, *Journal of membrane science* **2013**, *448*, 34.

[13] M. J. Raaijmakers, M. A. Hempenius, P. M. Schön, G. J. Vancso, A. Nijmeijer, M. Wessling, N. E. Benes, *Journal of the American Chemical Society* **2013**, *136*, 330.

[14] L.-Y. Chu, S. Wang, W.-M. Chen, *Macromolecular Chemistry and Physics* **2005**, *206*, 1934.

[15] H. Furukawa, K. E. Cordova, M. O'Keeffe, O. M. Yaghi, *Science* **2013**, *341*, 1230444.

[16] Y. Hu, X. Dong, J. Nan, W. Jin, X. Ren, N. Xu, Y. M. Lee, *Chemical Communications* **2011**, *47*, 737.

[17] J. Zuo, T.-S. Chung, *Water* **2016**, *8*, 586.

[18] B.-H. Jeong, E. M. Hoek, Y. Yan, A. Subramani, X. Huang, G. Hurwitz, A. K. Ghosh, A. Jawor, *Journal of Membrane Science* **2007**, *294*, 1.

[19] N. Y. Yip, A. Tiraferri, W. A. Phillip, J. D. Schiffman, M. Elimelech, *Environmental science & technology* **2010**, *44*, 3812.

[20] M. Tian, C. Qiu, Y. Liao, S. Chou, R. Wang, *Separation and Purification Technology* **2013**, *118*, 727.

[21] L. Wang, M. Fang, J. Liu, J. He, J. Li, J. Lei, *ACS applied materials & interfaces* **2015**, *7*, 24082.

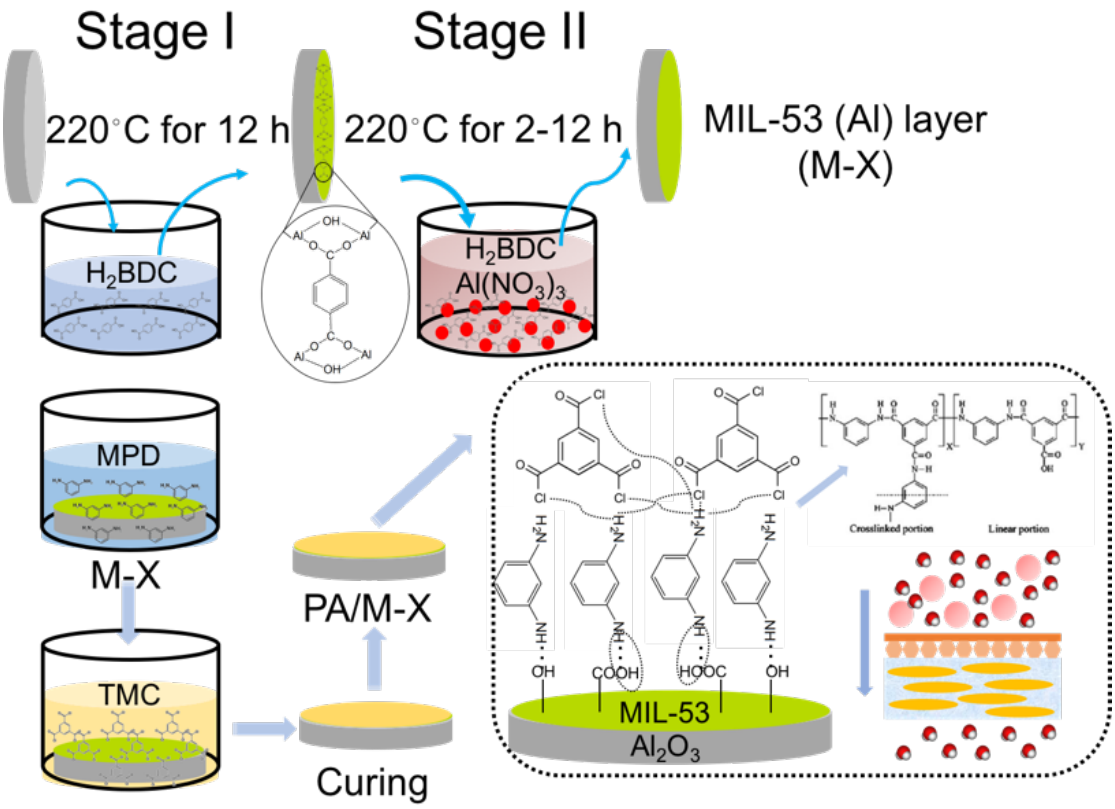

Figure 1. Schematic diagram of preparation of PA layer on Al_2O_3 substrate via a MOF-mediated IP method (X = the hydrothermal growth hours). M-X means MOF membrane at X h and PA/M-X means PA layer on MOF membrane at X h.

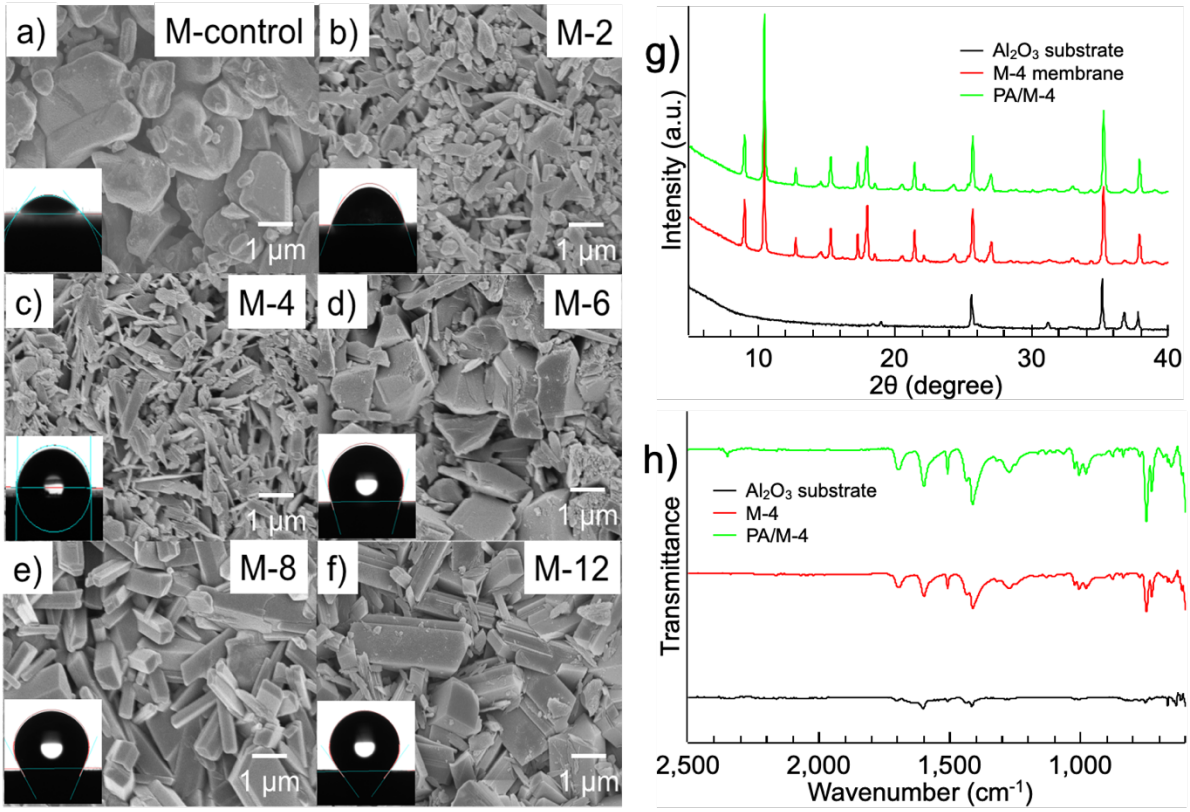

Figure 2. Characterization of M-X and PA/M-X membranes. (a-f, FESEM images of MIL-53 (Al) membranes (M-X); g) XRD patterns and h) FTIR spectra of the Al_2O_3 substrate, M-4 and PA/M-4.

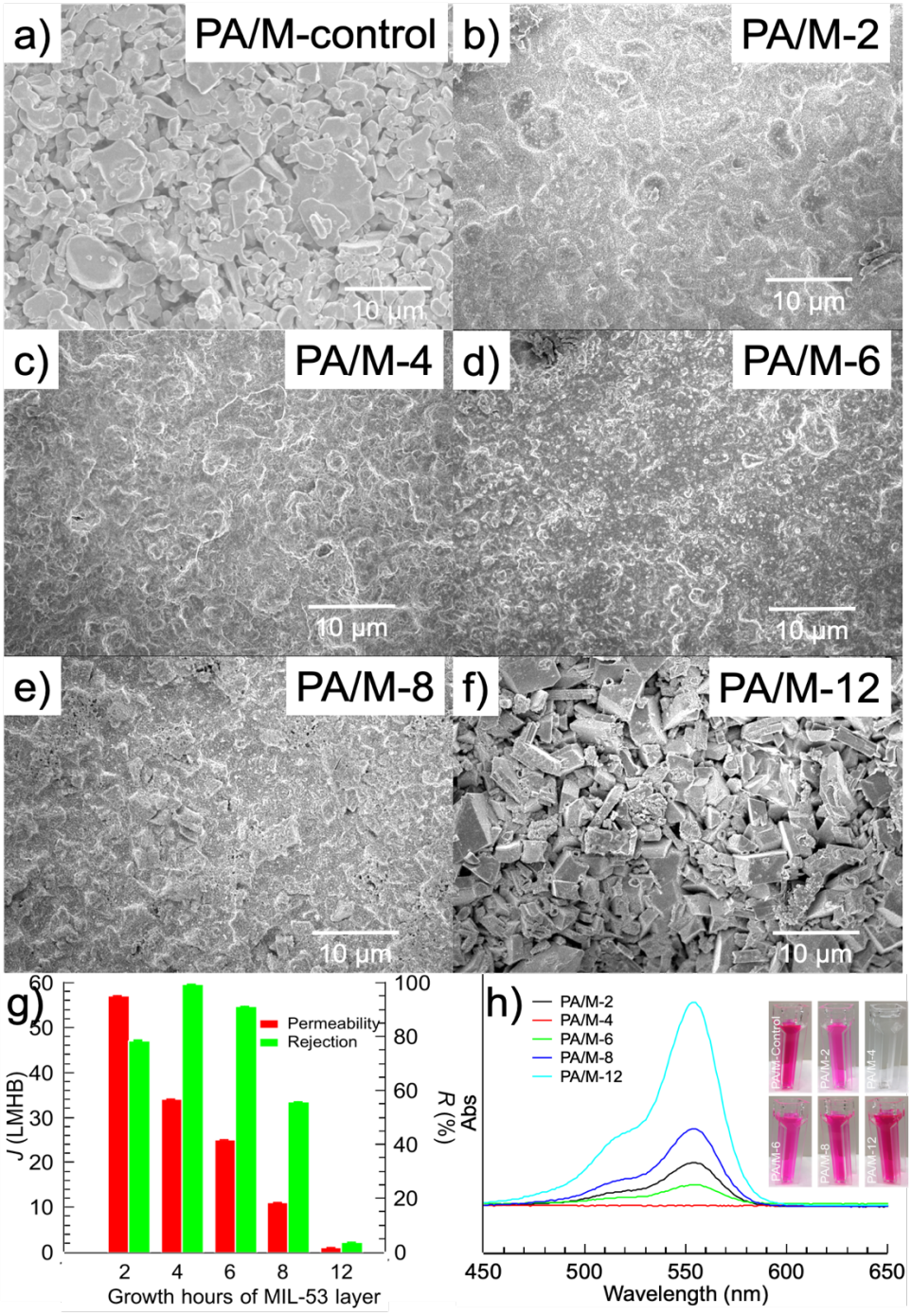

Figure 3. Characterization and performance evaluation of PA/M-X membranes (a-f, FESEM images of PA/MIL-53 (Al) membranes (PA/M-X); g, Pure water permeability and RhB rejections of PA/M-X; h, UV-Vis absorption spectra of permeate treated with different membranes.

A novel metal organic framework (MOF) - mediated interfacial polymerization for direct deposition of polyamide layer on ceramic substrates for nanofiltration

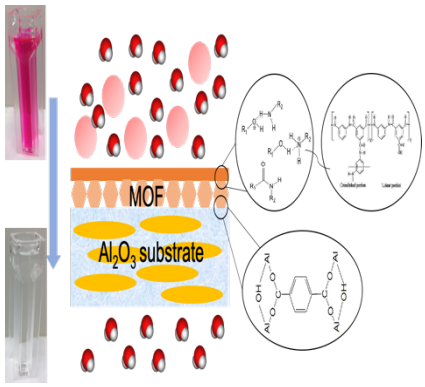

Supporting Information

A novel metal organic framework (MOF) - mediated interfacial polymerization for direct deposition of polyamide layer on ceramic substrates for nanofiltration

*Yueping Bao, Yunfeng Chen, Teik-Thye Lim, Rong Wang and Xiao Hu**

Text S1. The details on materials used in the experiment.

Aluminum nitrate nonahydrate ($Al(NO_3)_3 \cdot 9H_2O$), benzene-1,4-dicarboxylic acid ($C_8H_6O_4$, H_2BDC), benzene-1,3,5-tricarboxylic acid ($C_9H_6O_6$, H_3BTC), powder Al_2O_3 (100 mesh, 99%), *m*-phenylenediamine ($C_6H_8N_2$, MPD), trimesoyl chloride ($C_9H_3O_3Cl_3$, TMC), *n*-hexane and Rhodamine B ($C_{28}H_{31}ClN_2O_3$) were purchased from Sigma-Aldrich. Sodium chloride (NaCl) and magnesium sulfate ($MgSO_4$) were from Merck. All chemicals were of reagent grade or higher and were used without further purification. All solutions were prepared in deionized (DI) water (18.2 MΩ.cm at 25°C) from a Milli-Q purification system.

Porous Al_2O_3 ceramic substrates used in the experiments were provided by Nanjing Shuyihui Scientific Instruments CO., LTD (Nanjing, China). The substrates are disc-shaped with a pore size of ~100 nm. The diameter of the substrate is 22 mm and the thickness is 2 mm. One side of the ceramic substrate was polished by SiC sandpaper and washed with DI water before being used for the growth of MOF layer.

Text S2. Characterization techniques.

A field emission scanning electron microscope (FESEM, JSM-7600F, JEOL) was used for the evaluation of membrane morphology and the membrane surface roughness was measured by atomic force microscopy (AFM, Cypher S, Asylum Research). The vibrational absorbance and structural characteristics of as-prepared composites were investigated by Fourier transformed infra-red spectrometer (FTIR, Perkin Elmer). The mineralogy and crystal

structures of composites were analysed using X-rays diffractometer (XRD, Bruker D8 Advance) with a monochromatic high intensity Cu-K_α (λ =1.54 Å) radiation over a 2θ range of 5-40° at a step size of 0.02 combined with a rotation speed of 15 rpm. The chemical bonding analysis was conducted by X-ray photoelectron spectroscopy (XPS) on a Kratos Axis Supra spectrophotometer (Shimadzu) equipped with a dual anode monochromatic Kα excitation source (hv = 1486.7 eV).

Text S3. The details for home-made membrane filtration tests.

The membrane filtration tests are conducted in a home-made dead-end membrane filtration system (shown as **Figure S3**). The transmembrane pressures (TMP) in clean water permeate flux experiments were varied in the range of 1-10 bar. The mass of permeate was measured and converted to permeate flux according to the **Equation. S1**.

$$J = V / \mathrm{A}\, t \qquad \textbf{(S1)}$$

where J represents permeate flux (LMH, $Lm^{-2}\ h^{-1}$), V is volume of permeate (L), A is effective membrane surface area (m^2), t represents the filtration time (h), ΔP means the transmembrane pressure (TMP, Pa)

In the rejection test, the applied trans-membrane pressure is 10 bar and the feed (RhB, $MgSO_4$ and NaCl) concentration is 100 mg L^{-1}. The stabilization time is 2 hours before sampling. And the concentration of RhB, $MgSO_4$ and NaCl in the permeate side was determined by UV-1800 spectrophotometer (Shimadzu, Japan) and conductivity meter (Myron L).

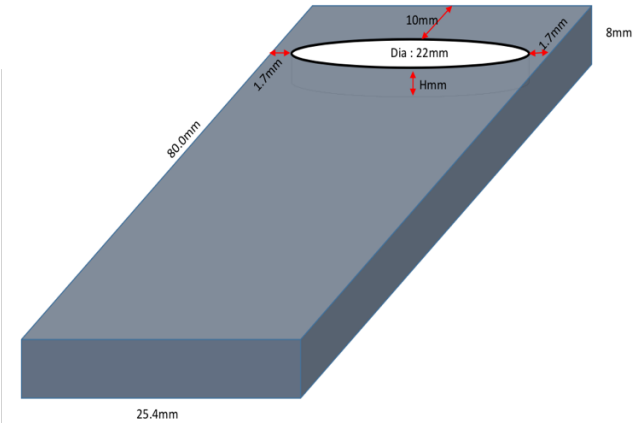

Figure S1. The sample holder of ceramic substrates for seed growth.

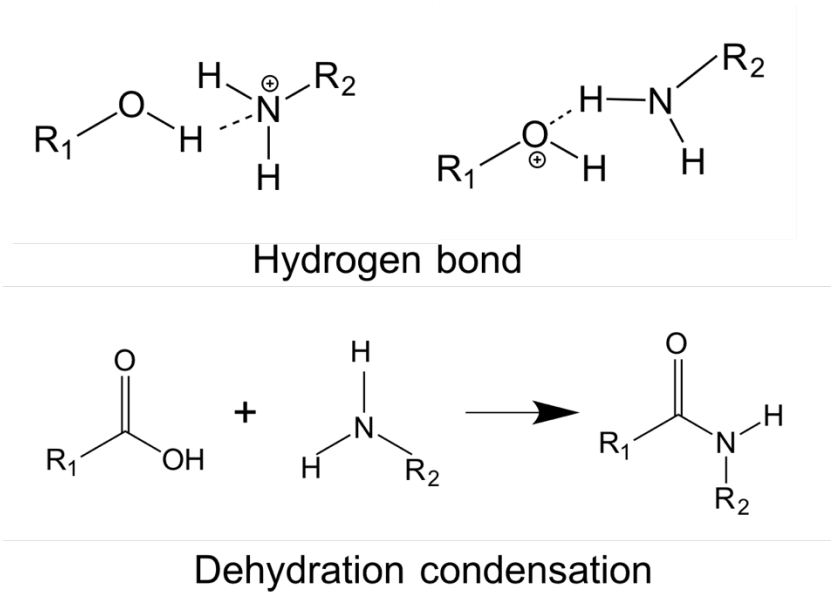

Figure S2. The chemical reactions between -OH/-COOH in MIL-53 (Al) and -NH_2 in MPD via hydrogen bond and dehydration condensation.

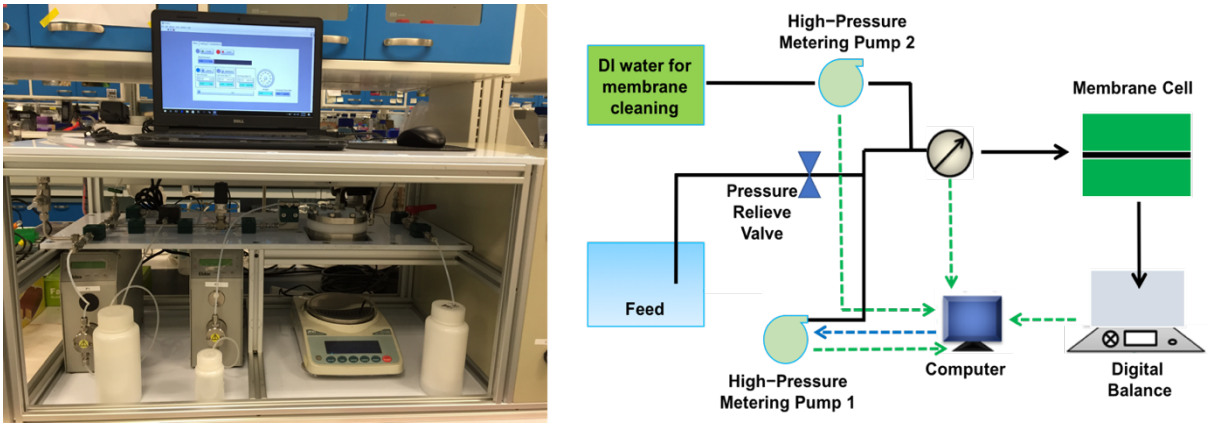

Figure S3. The home-made membrane filtration system.

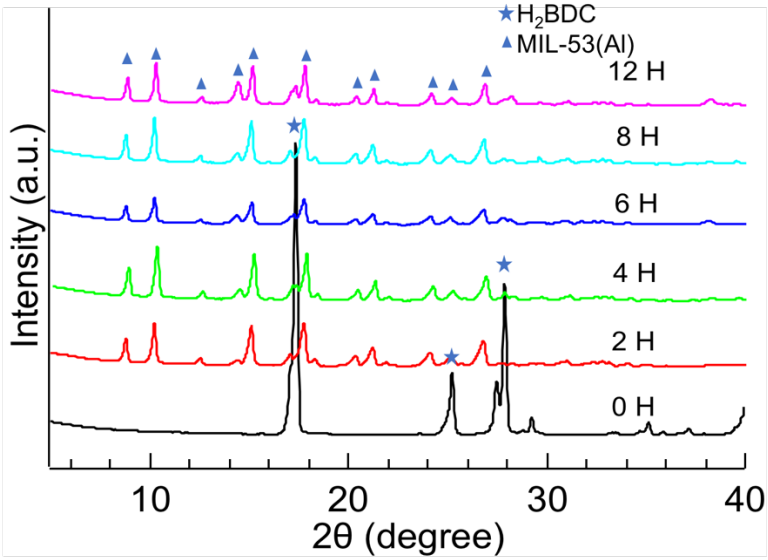

Figure S4. XRD patterns of as-prepared MIL-53 particles with different hydrothermal hours.

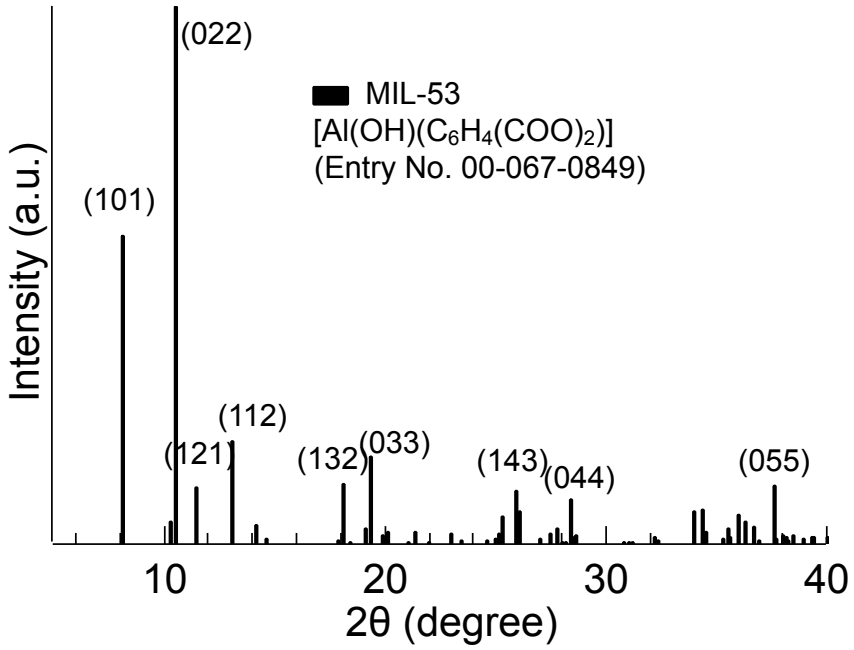

Figure S5. The simulated XRD patterns for MIL-53 (Al).

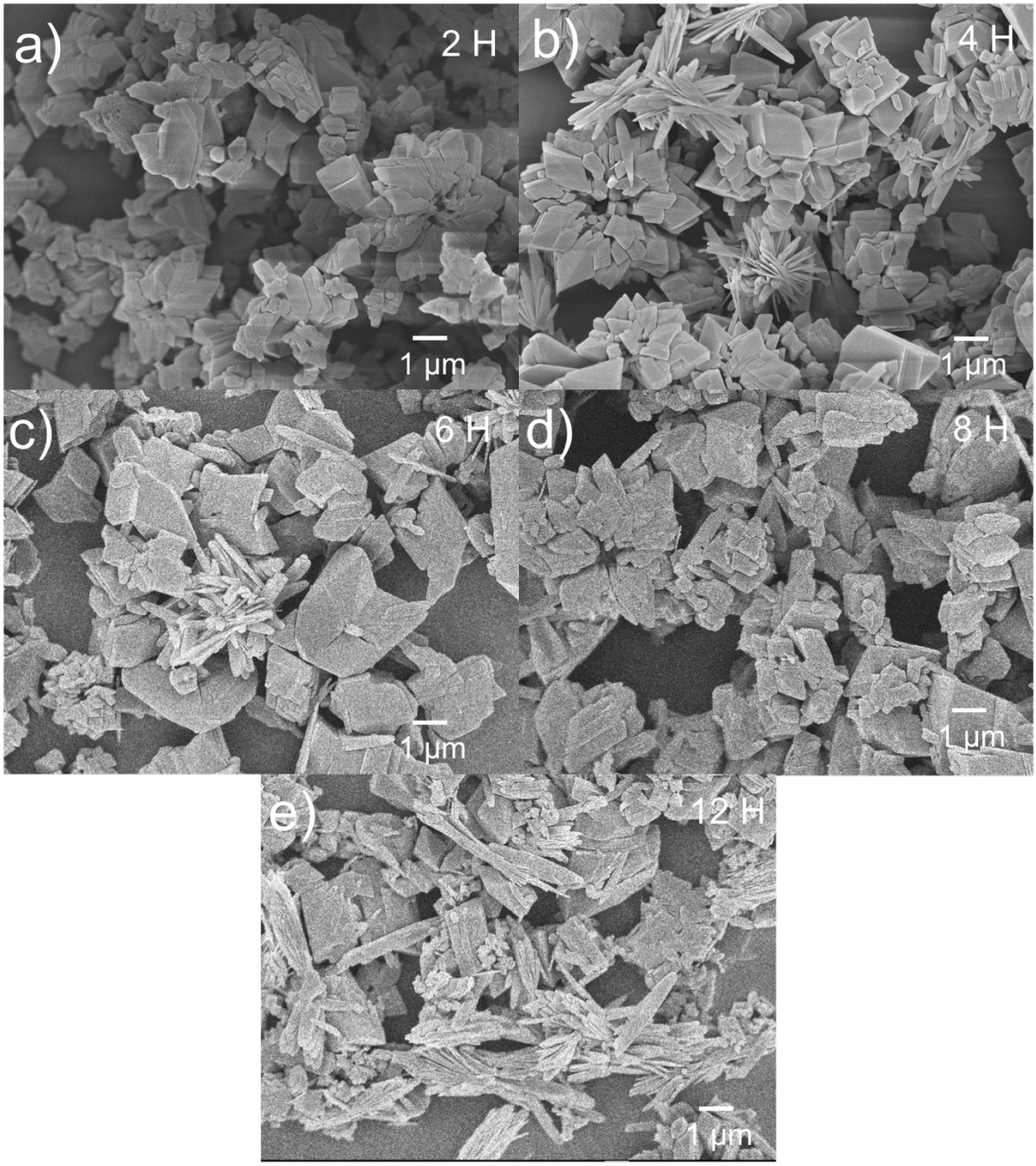

Figure S6. FESEM of MIL-53 powders prepared under different hydrothermal hours (2 h-12 h).

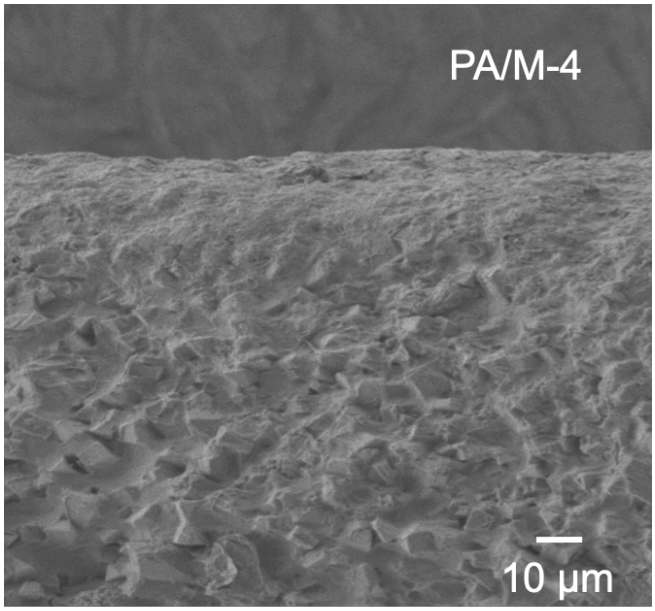

342

343 **Figure S7.** FESEM image of cross sections of PA/M-4.

344

345

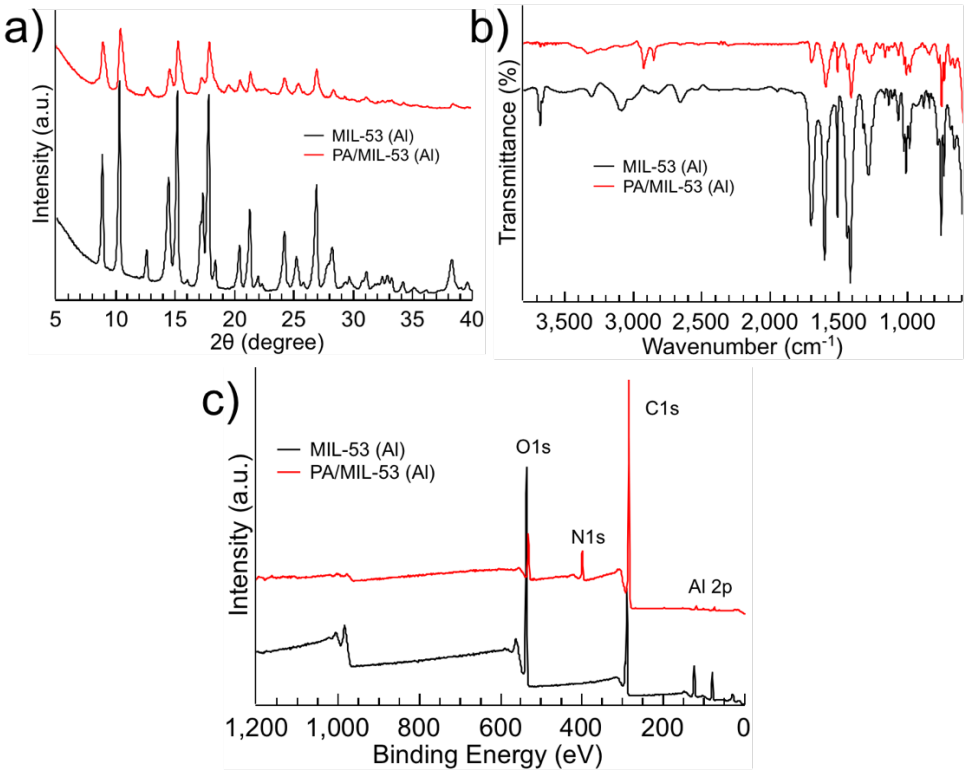

346

347 **Figure S8.** XRD patterns (a), FTIR spectra (b) and XPS wide scan (c) of MIL-53

348 powder (prepared at 12 h) and PA/MIL-53.

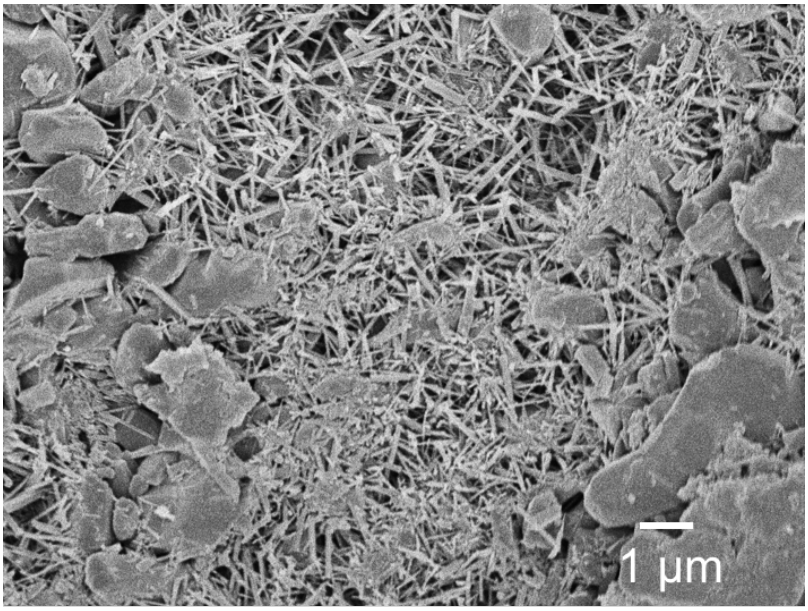

Figure S9. FESEM of seed layer on the Al_2O_3 surface.

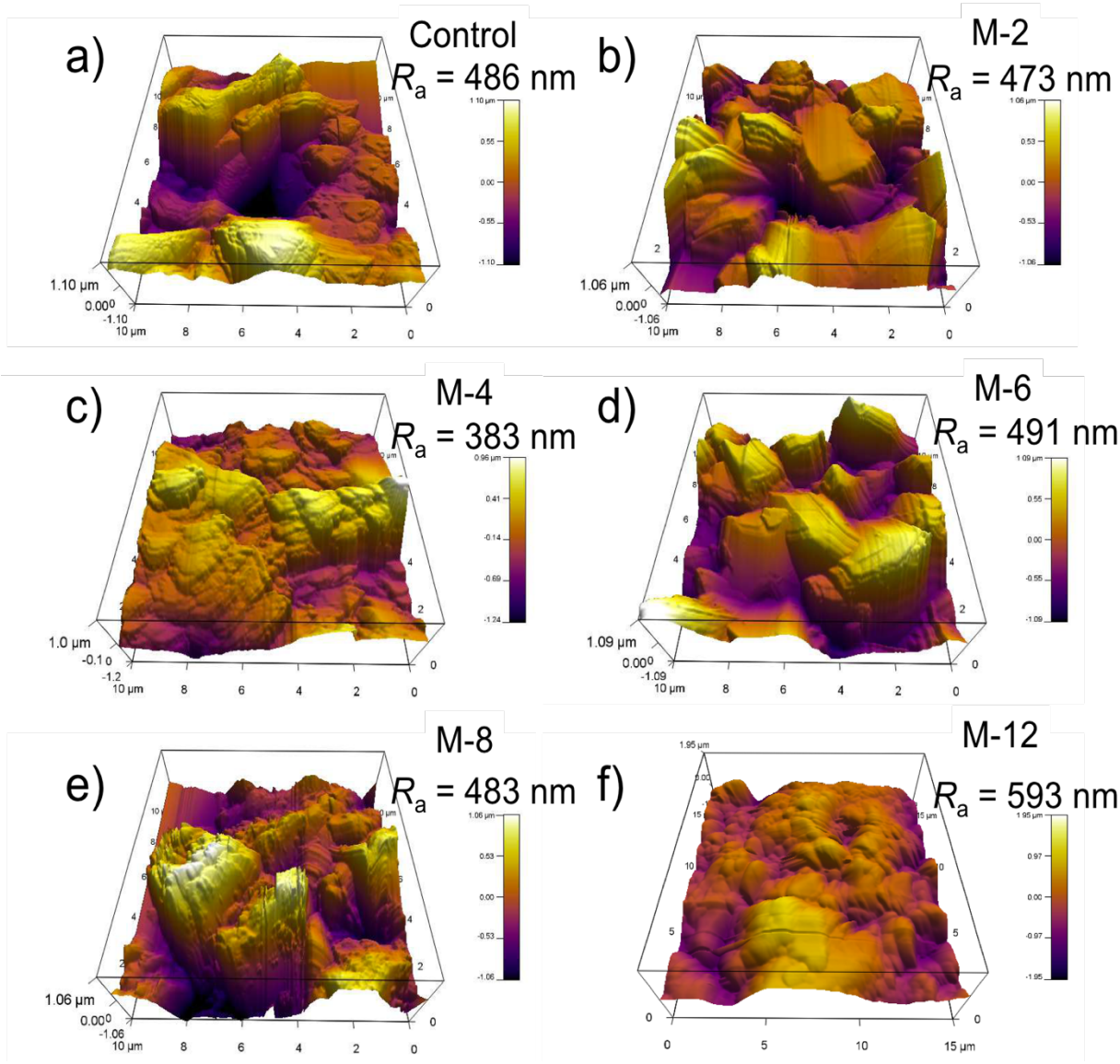

Figure S10. AFM of M-X prepared with different hydrothermal hours (X=2, 4, 6, 8 and 12).

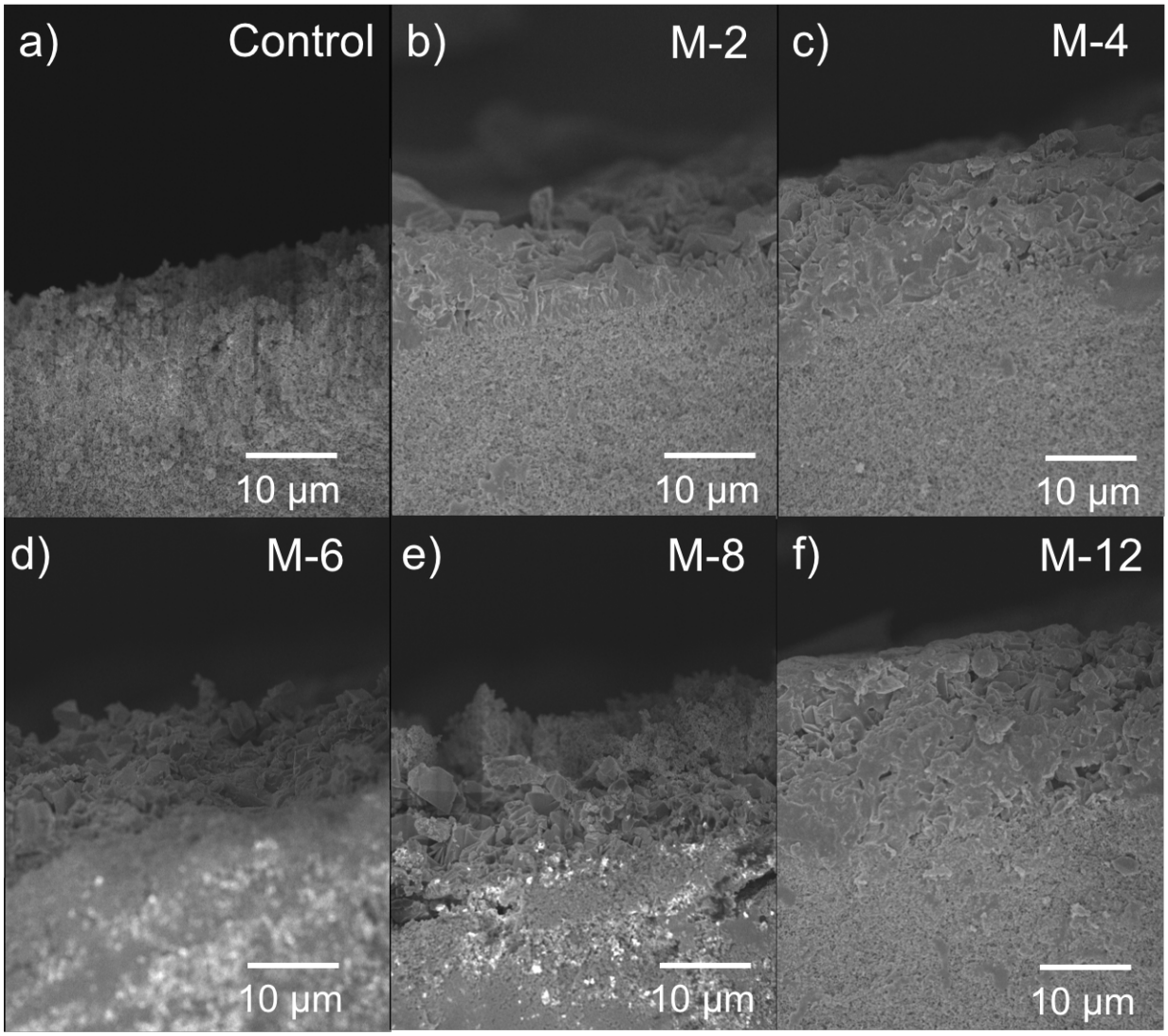

Figure S11. FESEM images of cross sections of M-X prepared with different hydrothermal hours (X=2, 4, 6, 8 and 12).

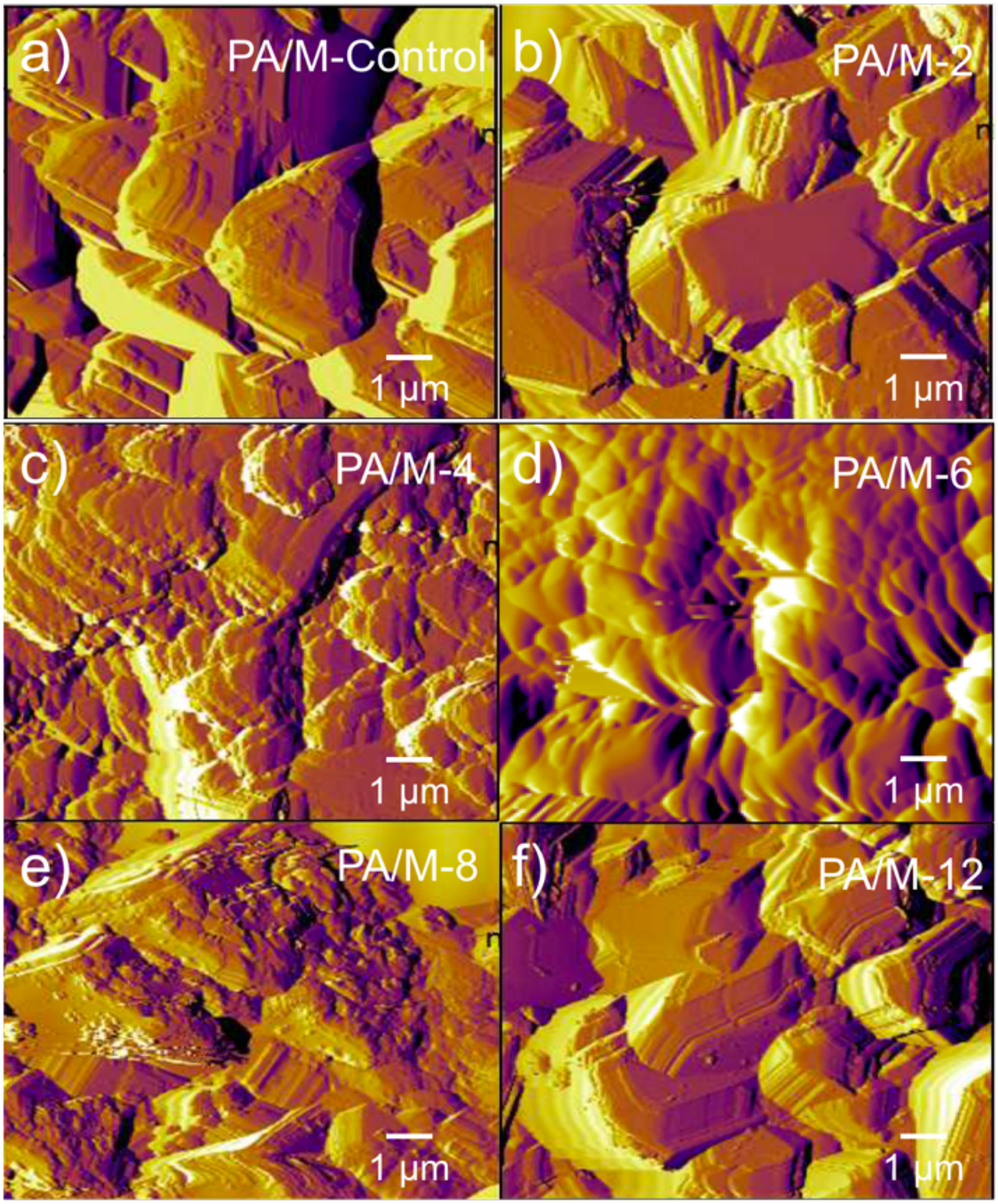

Figure S12. AFM images of PA/M-X (X means the growth hours).

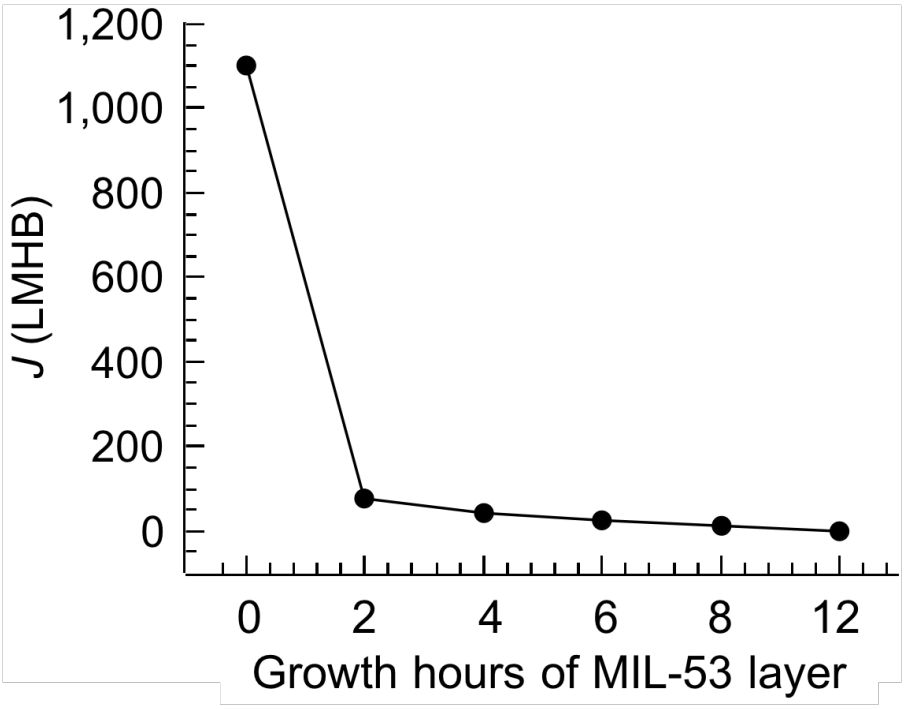

372

373 **Figure S13.** Pure water flux of M-X (X means the growth hours).

374

375

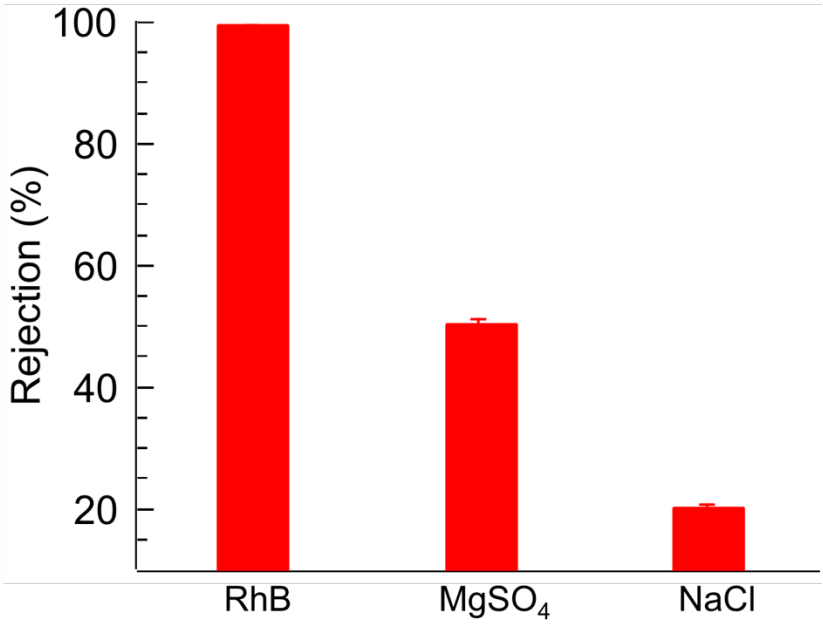

376

377 **Figure S14.** The rejection on different feed solution for PA/M-4.

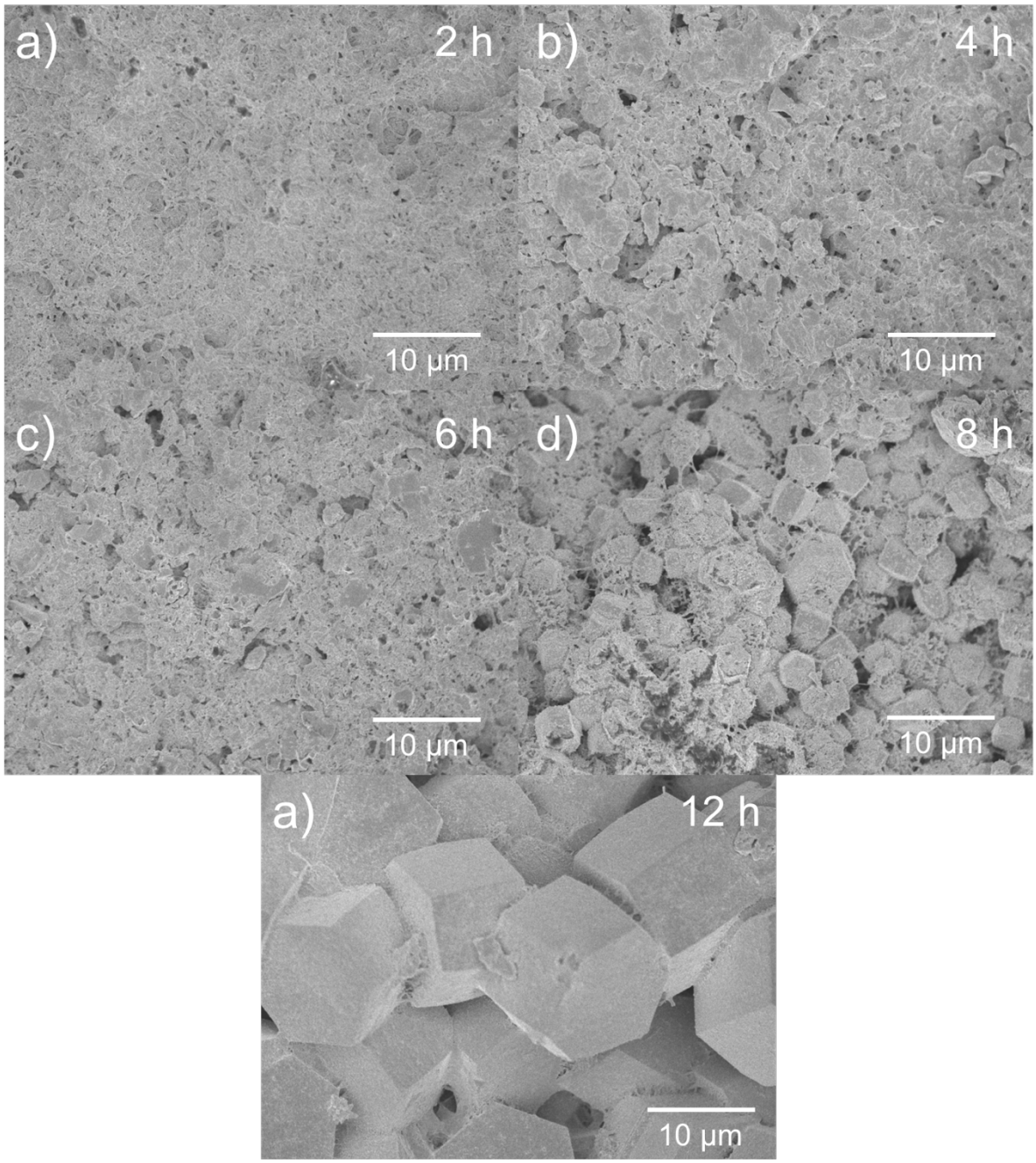

Figure S15. FESEM images of polyamide layer on MIL-93 modified ceramic substrates with different hydrothermal hours (X=2, 4, 6, 8 and 12).